Structural Durability & Health Monitoring

Tech Science Press

Doi:10.32604/sdhm.2025.075327 Published Online: 18 December 2025

ARTICLE

Experimental Validation on a Real-World Truss Structure of a Damage Localization Method Based on Mode Shape Derivatives

Giada Faraco*, Andrea Vincenzo De Nunzio, Nicola Ivan Giannoccaro* and Arcangelo Messina

Department of Innovation Engineering, University of Salento, Lecce, 73100, Italy

*Corresponding Authors: Giada Faraco. Email: giada.faraco@unisalento.it; Nicola Ivan Giannoccaro. Email: ivan.giannoccaro@unisalento.it

Received: 29 October 2025; Accepted: 03 December 2025

ABSTRACT: Damage detection and localization analysis have gained increasing importance over the years, due to the growing number of catastrophic events and the associated risks that small, undetected cracks in structures may evolve into severe failures if not identified in time. In this context, vibration-based methods have been extensively investigated for structural damage detection. Among them, one of the most widely used approaches since its introduction is the curvature method. It has been successfully employed in numerous studies, consistently providing reliable results. However, the use of second-order or higher-order derivatives can be challenging when dealing with experimental data, as these are highly sensitive to measurement noise. Conversely, using the first derivative may simplify the analysis while maintaining robustness. Therefore, the present work introduces and experimentally demonstrates an extension of the curvature-based approach, focusing on the integration of the first derivative for damage localization. In particular, both methods based on the use of the second and first derivatives were applied to detect their capability in detecting and localizing the damage. This was tested on a slender truss structure, with induced damages at different locations, equal to just 1.069% of the structure volume. The results, obtained from this real-world case study, show that for certain structures, like slender ones, the use of the first derivative can achieve equal or even superior damage detection performance compared to the traditional second derivative method. Specifically, the comparison was evaluated based on the accuracy in localizing the damage with the two methods, both from a visual and quantitative point of view, since a deviation index δ was also introduced.

KEYWORDS: Damage localization; mode shapes; mode shape derivatives; curvature method; structural health monitoring

1 Introduction

Over the years, Structural Health Monitoring (SHM) has gained increasing importance as a means to prevent structural failures that can lead not only to economic losses but, more critically, to the loss of human life. Unfortunately, the literature reports numerous catastrophic events, both in civil and mechanical engineering contexts, that have resulted in significant damage and casualties.

Although certain cases—such as the failure of an electrical transmission tower—might appear less critical at first glance, such events can have extensive consequences. Indeed, the collapse of a single electric tower, which is often subjected to harsh environmental conditions and various types of degradation, can cause the failure of an entire power line and so major disruptions to economic activity and everyday life [1].

To mitigate such risks, it is essential to apply preventive damage detection analyses and to develop methods that are both simple and rapid, ensuring timely intervention when continuous monitoring is not feasible.

Over the past decades, a vast number of approaches have been proposed across different research fields. Among them, vibration-based methods have proven to be particularly effective for SHM and damage detection due to the high sensitivity of modal parameters to structural deterioration. Specifically, several techniques have been developed based on changes in natural frequencies, mode shapes, modal strain energy, modal flexibility, matrix updating (stiffness and mass), and various nonlinear approaches [2,3].

In recent years, several authors have shown increasing interest in combining modal parameters for damage detection with methods from other research fields. For instance, one rapidly growing area is the integration of Artificial Intelligence (AI) techniques into SHM applications [4], or the use of Convolutional Neural Networks (CNN) [5,6]. The Statik and Dynamik research group at Leibniz University Hannover has also explored, for example, on a real-world structure, the use of artificial neural networks and autoencoders in particular [7], as well as transfer learning techniques to transfer damage-related information, based on modal features, from a source structure with known damage to a target structure without such information, enabling a more complete dataset for both [8]. They have also investigated a multi-objective optimization approach combined with stochastic model updating for damage localization [9] and the application of the autocovariance function in this context [10].

These studies are cited here merely as representative examples, illustrating how this line of research has become increasingly active, with many other groups worldwide exploring similar hybrid approaches.

Nevertheless, although these methods have shown promising results, they often require significant computational effort, as well as reference data or supporting simulations. In addition, such approaches typically demand considerable time to train complex algorithms or to perform model-updating procedures. Unfortunately, this time is not always available in practical applications, where prompt detection and intervention are crucial to ensure structural safety and prevent further deterioration.

Within this framework, one of the vibration-based methods that has attracted considerable attention due to its simplicity, low computational cost, and minimal data requirements is the curvature method, first introduced by Pandey et al. [11]. This technique relies solely on the measurement of a displacement field associated with the structural response. Based on the relationship between structural stiffness and curvature, the method involves extracting the structure's mode shapes and computing their second derivative, which can be estimated using finite difference schemes [11,12] or enhanced through other tools, such as the Continuous Wavelet Transform (CWT). The latter approach, as demonstrated by [13,14], significantly improves the accuracy and robustness of curvature estimation.

Regardless of the specific computational technique employed, the curvature method enables fast and effective damage localization without requiring a reference dataset, numerical model, or destructive testing. For these reasons, this approach has been extensively investigated, resulting in a large body of literature.

Among all the published works, some curvature-based techniques employ a reference model or data of the undamaged structure, using damage indices that compare the healthy and damaged states. They have been widely tested in either numerical [15–17] or experimental studies [18–22]. However, such information is often unavailable, especially in the case of historical structures or aging mechanical components, where no prior data exists. Therefore, it is essential to expand and refine reference-free approaches. Other authors have tested the curvature method under a variety of conditions [23–25], and even extended it by using higher-order derivatives (e.g., third and fourth derivative-based methods) [26,27].

Nevertheless, the curvature method has been widely employed and adapted in numerous studies, leading to the publication of a substantial number of papers in the field.

Hoping that a concise overview of the most relevant contributions has been provided, the aim of the present work is to demonstrate, through a real-world case study, that an extension of the curvature method, toward the use of the first derivative alongside the traditional second derivative (as previously introduced and discussed by the authors in another study), can also be of significant interest.

This is especially relevant since the first derivative is generally easier to estimate than higher-order derivatives, which are more sensitive to experimental noise. In some previous works, the first derivative has been incorporated into damage detection analyses, typically through specific damage indices that also depend on the second derivative, thereby increasing computational time. Alternatively, if used alone, the first derivative was mostly tested with information related to a reference healthy state, in numerical simulations, or on beam or plate-like structures [28–31].

Therefore, the objective of this study is to demonstrate the applicability and the necessity of using this extended approach, showing—through a real-world experimental dataset rather than a simulated one—that the use of the first derivative of the torsional mode shape can lead to simpler and more effective results, depending on the structure's characteristics and geometry. Furthermore, the method retains the key advantages of being reference-free and non-destructive, making it particularly suitable for practical SHM applications.

The manuscript is organized as follows: first, a theoretical description of the proposed and applied method is provided. Section 3 presents the real-world case study and the corresponding experimental campaign, while Section 4 discusses the obtained damage localization results. Finally, the main conclusions are drawn.

2 Method

It is well known that the second derivative of the mode shape is sensitive to damage localization, as it reflects the relationship between variations in structural stiffness and curvature.

Specifically, consider a beam with a circular cross-section undergoing pure bending deformation and subjected to a continuous bending moment. At a given instant in time, the following equation Eq. (1) can be expressed:

$$\chi(x) = \upsilon''(x) = \frac{M_b(x)}{EJ} \tag{1}$$

where M_b is the bending moment, E represents Young's modulus, and J is the geometric moment of inertia of the beam's cross-section. Damage at a specific cross-section of the beam results in a local reduction of bending stiffness, leading to a change in the structural curvature $\chi(x)$ at that location. As the curvature can be described through the use of the second derivative, this effect becomes evident through the appearance of a sudden peak in the second derivative of the mode shape, $\upsilon''(x)$, at the damage position [11]. In fact, Eq. (1) shows a clear inverse proportionality between the structure stiffness and the second derivative.

Similarly, an equation analogous to Eq. (1) can be derived for a beam with a uniform circular cross-section subjected to a continuous external torque $M_t(x)$. In particular, the theory of pure torsion states that in this case, the torsion angle $\theta(x)$ per length unit x, is directly related to the applied continuous torque $M_t(x)$ and the torsional rigidity GJ_0 as shown in Eq. (2) [32]:

$$\frac{\theta(x)}{x} = \frac{M_t(x)}{GJ_0} \tag{2}$$

Therefore, when damage occurs at a generic cross-section of the beam, the resulting sudden reduction in torsional stiffness produces a corresponding discontinuity in the rotation angle $\theta(x)$, as described in Eq. (2). By evaluating how $\theta(x)$ varies along the beam through its first derivative, Eq. (3), it becomes possible to observe a distinct peak in the derivative curve. This peak reliably indicates the location of the stiffness change and thus the position of the damage.

$$\frac{\mathrm{d}\theta\,(x)}{dx} = \frac{M_t(x)}{GJ_0} \tag{3}$$

This implies that, in the case of pure torsional deformation of the beam, through Eq. (3) a relation equivalent to the one described by the curvature method can be derived, leading to the same result in damage localization but analyzing the pure torsional mode that is directly related to the rotation (θ) of the structure. Therefore, similarly to the bending case, which was the most commonly used and the only one originally introduced by Pandey et al. [11], considering Eq. (3) extends the concept to situations in which torsion is the dominant deformation mechanism, making it applicable to torsional mode shapes as well.

This extension is particularly important because pure bending modes are not always guaranteed in real-world structures. Geometric and material characteristics may lead to predominantly bending or torsional modes, or even to coupled flexural–torsional modes in which one component prevails over the other. Therefore, it becomes essential to also consider the relationship described in Eq. (3) and to carefully evaluate each case. When bending deformation dominates the mode shapes, the curvature method is appropriate, whereas when torsion is predominant, the first-derivative method should be employed [33].

Moreover, the lower sensitivity of the first derivative, compared to the second, in exhibiting spurious peaks due to noise in the measured data must be taken into account. Therefore, it is essential to employ both approaches when dealing with structures that exhibit bending, torsional, or even coupled behaviors, and to carefully analyze and select the most reliable results.

Therefore, the main objective of this work is to demonstrate the validity of this approach using data acquired from a real-world structure and, in particular, to highlight the advantages of employing the first derivative instead of the second one for damage localization in the tested structure.

The structure under investigation, described in detail in Section 3, is a slender truss structure. Consequently, it can be reasonably approximated by a beam with a circular cross-section. In this context, it is worth noting that the rotation $\theta(x)$ corresponds to the tangential displacement $w(x)$, up to a constant equal to the radius R of the beam's cross-section, according to $w = R\theta$. Hence, the rotational displacement fields were approximated by the axial displacements $w(x)$.

Moreover, in this study, both Eqs. (1) and (3) were calculated aided by the use of CWTs (Continuous Wavelet Transforms). This choice is because derivatives and CWT have similar performance, and they cannot be considered two distinct and completely different mathematical tools. Moreover, they showed better performance in the case of data corrupted by external noise [13,14]. Eq. (4) shows the relations utilized.

$$\begin{cases} \dfrac{dy}{dx} \approx kh_1 * y \\ \dfrac{d^2y}{dx^2} \approx kh_1 * (h_1 * y) \end{cases} \tag{4}$$

where the symbol "$*$" denotes the numerical convolution operator between two finite sample streams (h_1 and y), h_1 is the differentiator filter, and y is the data stream.

3 Case Study

The method was tested on a real-world structure, the Leibniz University Test Structure for MOnitoring (LUMO). This structure was made available by the Institute for Statics and Dynamics (ISD) research group of Leibniz University Hannover, and is used for experimental validation of Structural Health Monitoring (SHM) methods [34].

3.1 Structure and Experimental Setup Description

The structure is a 9-m-tall steel lattice truss. It is installed outdoors, approximately 20 km south of Hanover (Lower Saxony, Germany), and is therefore exposed to natural environmental conditions and ambient excitation (Fig. 1) [35].

Figure 1: LUMO structure photo

A distinctive feature of the LUMO structure is its capability to introduce reversible damage at six different levels, three of which are the focus of this study and illustrated in Fig. 2, denoted as D1, located between 0 and 1 m of the tower height, D2 situated between 3 and 4 m, and D3 between 4 and 5 m. These configurations are achieved through a reversible mechanism that allows the disconnection of single or multiple bracings, resulting in a localized reduction of stiffness and mass. For this study, each damage, at every location (D1, D2, and D3), was obtained by disconnecting three braces at the same time, resulting in a damage entity of 1.069% of the entire volume of the structure.

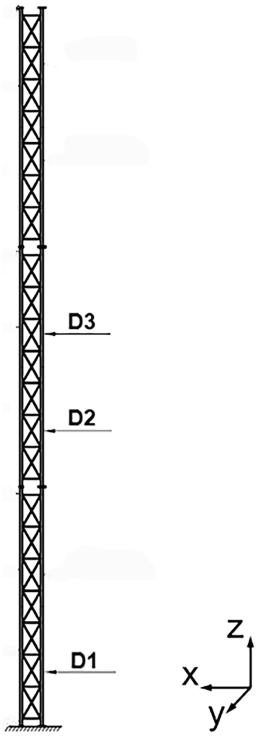

Figure 2: Tested damage positions on the LUMO structure

Also, a new measurement setup was installed on the LUMO structure. It was equipped with 32 accelerometers placed (ML1, ML1.1, ML1.2, ML1.3, ML2..., ML9, ML9.1, ML9.2 in Fig. 3a) on leg 1 (see Fig. 3b) and all of them oriented to acquire in the *y* direction, as visible from the structure's top view in Fig. 3b, in order to acquire just the axial movements of the structure. In Fig. 3a, the new accelerometers are displayed with blue arrows, while the red ones indicate the sensors already installed on the structure and used for previous studies.

Due to structural impediments, the sensors were not placed perfectly equispatially. Their placement height is reported in Table 1.

Each dataset used for the damage detection analysis was obtained from just 10 min of acquisition, for each damaged case, with a sampling frequency of 1200 Hz.

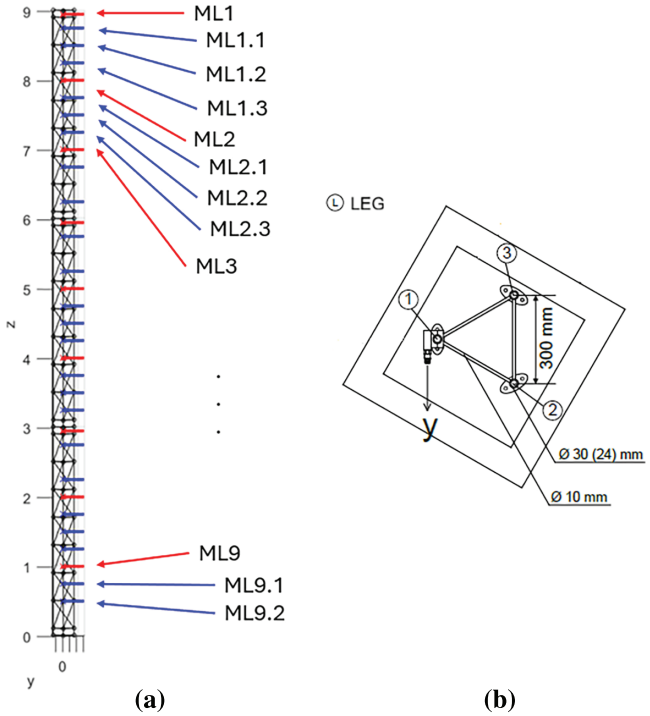

Figure 3: Sensors placement shown in plane *yz* (**a**) and orientation (**b**). Numbers 1 to 3 in (**b**) indicate the three different legs that make up the structure: sensors were placed on leg 1, sensors cables were placed on leg 2

Table 1: Sensors placement on LUMO structure

Accel.	**ML1**	**ML1.1**	**ML1.2**	**ML1.3**	**ML2**	**ML2.1**	**ML2.2**	**ML2.3**	**ML3**	**ML3.1**	**ML3.2**
Height [m]	8.95	8.60	8.46	8.23	8.00	7.88	7.60	7.23	7.00	6.71	6.40
Accel.	**ML4**	**ML4.1**	**ML4.2**	**ML5**	**ML5.1**	**ML5.2**	**ML5.3**	**ML6**	**ML6.1**	**ML6.2**	**ML6.3**
Height [m]	5.95	5.64	5.35	5.00	4.79	4.54	4.23	4.00	3.82	3.58	3.30
Accel.	**ML7**	**ML7.1**	**ML7.2**	**ML8**	**ML8.1**	**ML8.2**	**ML8.3**	**ML9**	**ML9.1**	**ML9.2**	
Height [m]	2.95	2.64	2.32	2.00	1.77	1.50	1.23	1.00	0.73	0.40	

3.2 Obtained Mode Shapes

The analysis focused on the first three mode shapes obtained using the new setup implemented on the structure. Specifically, these modes include two flexural and one torsional mode shape, illustrated in Fig. 4a–c, for all the damage cases. They were extracted during a preliminary processing phase performed with the ARTeMIS Modal software [36], using Operational Modal Analysis (OMA) techniques such as the Stochastic Subspace Identification (SSI) method.

As expected, the mode shapes exhibit oscillations resulting from the spatial discretization of the measurement setup, which was limited by both the number of available sensors and the geometric constraints of the structure.

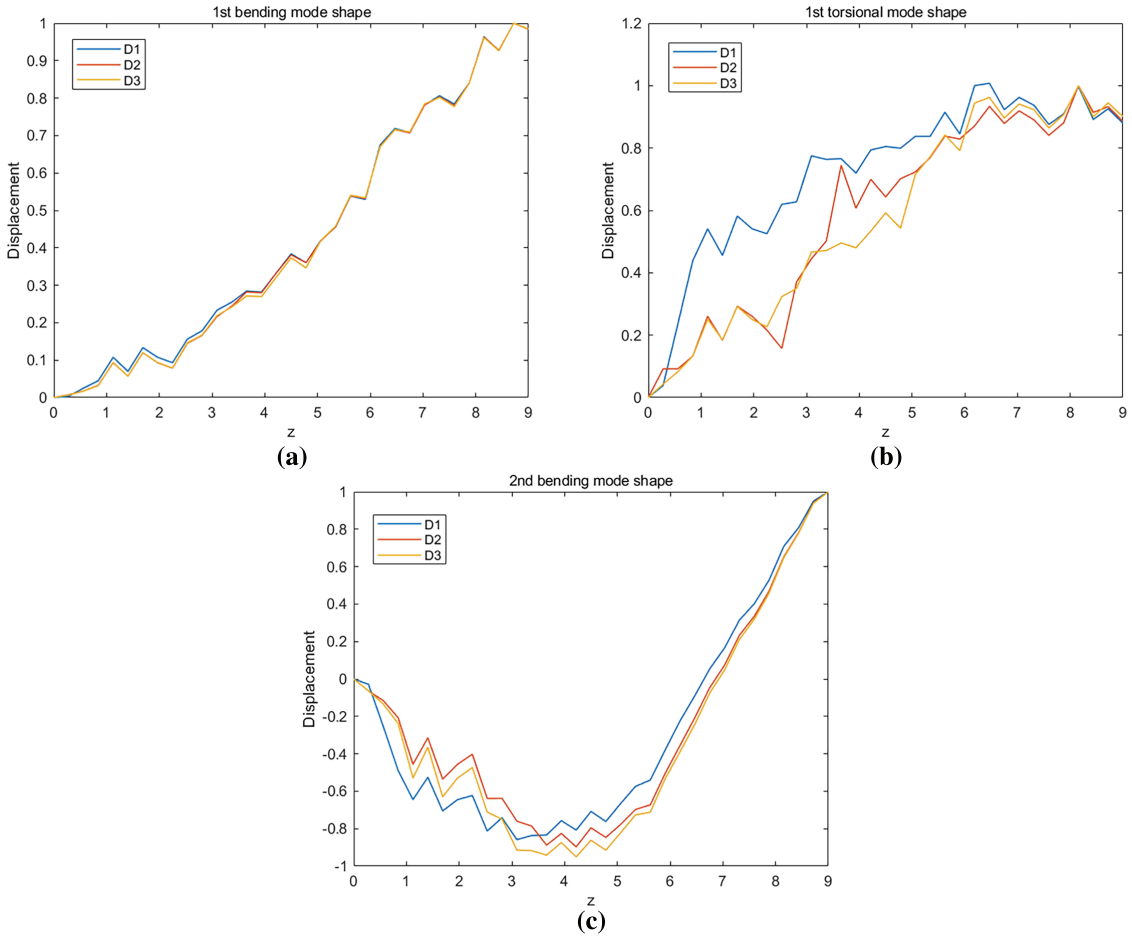

Figure 4: First three experimental mode shapes for the three damage cases: 1st bending (**a**), 1st torsional (**b**), and 2nd bending (**c**) mode shape

To verify that the newly acquired mode shapes are consistent with the theoretical ones and therefore suitable for subsequent analyses, a comparison was performed using the Modal Assurance Criterion (MAC), obtained through Eq. (5).

$$MAC\left(\varphi_i \psi_j\right) = \frac{\left|{\varphi_i}^T \psi_j\right|^2}{\left({\varphi_i}^T \varphi_i\right)\left({\psi_j}^T \psi_j\right)} \tag{5}$$

where φ_i and ψ_j are the two mode shapes to be compared. The MAC ranges between 0 and 1, where 1 indicates a perfect match between mode shapes and 0 indicates no correlation [37,38].

The experimentally obtained mode shapes from all damage cases were compared with the numerical mode shapes derived from a validated Finite Element (FE) model of the structure, in which an ideal configuration with 100 evenly spaced acquisition points was assumed, producing smooth reference mode shapes (Fig. 5a–c). To enable the application of the MAC formula, these 100 numerical points were subsequently reduced to 32, matching the experimental sensor configuration and acquisition locations.

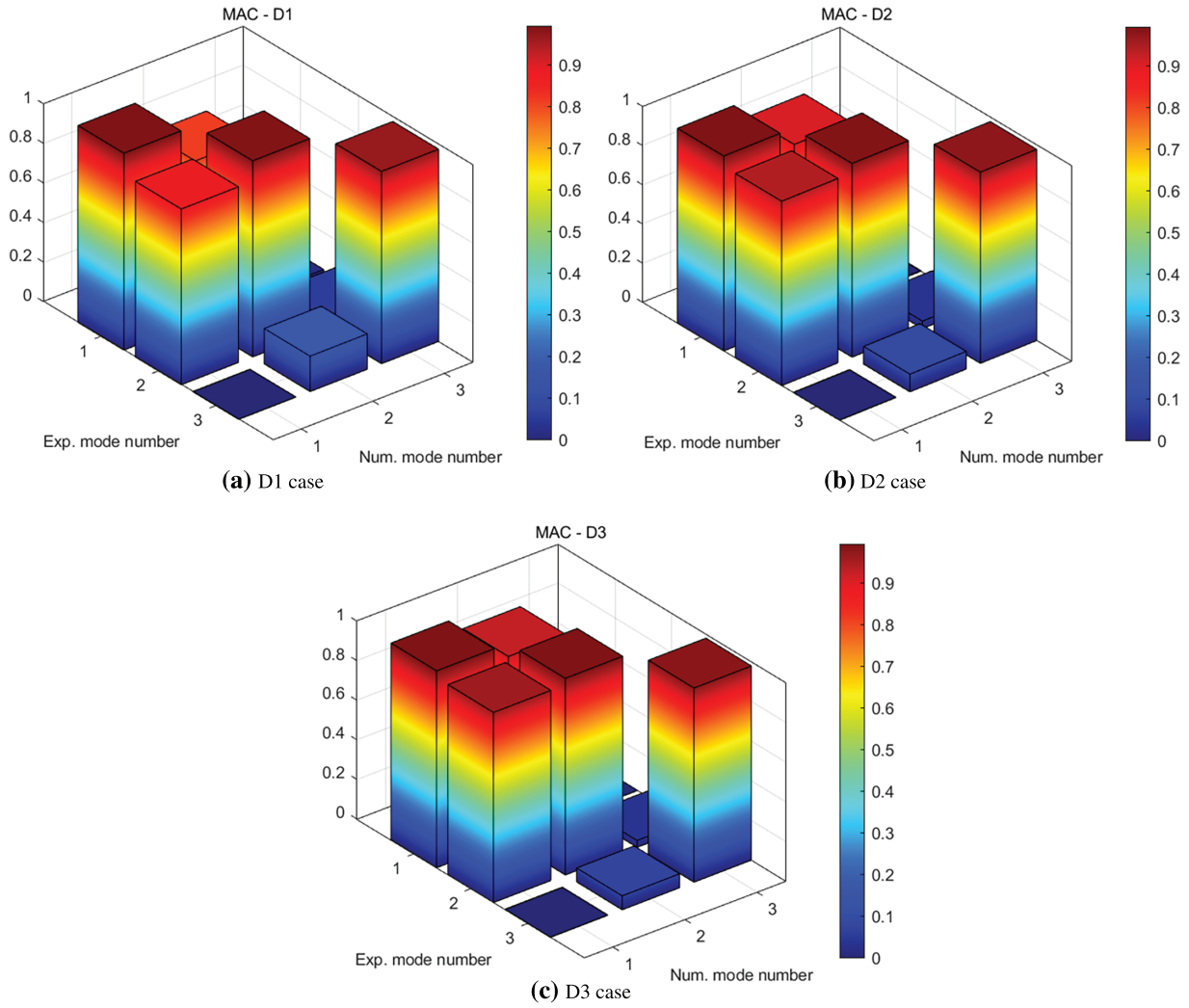

(a) D1 case **(b)** D2 case **(c)** D3 case

Figure 5: MAC results for the three damage cases between experimental mode shapes obtained with 32 acquisition points (labeled "Exp. Mode number") and numerical mode shapes obtained by simulating 100 acquisition points (labeled "Num. mode number"): (**a**) MAC for damage D1 case, (**b**) MAC for damage D2 case, (**c**) MAC for damage D3 case

Quantitative results are displayed in Tables 2–4.

Table 2: MAC values between the numerical mode shapes and the experimental ones for the D1 damage case

D1 Case		**Numerical**		
		1st Mode (bending)	**2nd Mode (torsional)**	**3rd Mode (bending)**
Experimental	**1st Mode (bending)**	0.9953	0.8152	0.0134
	2nd Mode (torsional)	0.8879	0.9910	0.0579
	3rd Mode (bending)	0.0015	0.1788	0.9715

Table 3: MAC values between the numerical mode shapes and the experimental ones for the D2 damage case

D2 Case		Numerical		
		1st Mode (bending)	2nd Mode (torsional)	3rd Mode (bending)
Experimental	1st Mode (bending)	0.9951	0.9086	0.0034
	2nd Mode (torsional)	0.9415	0.9887	0.0386
	3rd Mode (bending)	0.0019	0.0903	0.9760

Table 4: MAC values between the numerical mode shapes and the experimental ones for the D3 damage case

D3 Case		Numerical		
		1st Mode (bending)	2nd Mode (torsional)	3rd Mode (bending)
Experimental	1st Mode (bending)	0.9951	0.9282	0.0006
	2nd Mode (torsional)	0.9610	0.9939	0.0350
	3rd Mode (bending)	0.0021	0.0706	0.9813

As can be observed, despite the experimental mode shapes being derived from ambient excitation, affected by measurement noise, and obtained with only one third of the total acquisition points, there is a clear correspondence between the experimental and numerical first, second, and third mode shapes, with the MAC number in the diagonal almost equal to 1. While the elevated, though not unitary, MAC value between the first and second mode shapes, corresponding to the first bending and first torsional modes, arises from the natural similarity that characterizes these two shapes, as can also be observed in Fig. 4a,b.

Moreover, considering that 32 accelerometers represent a relatively large number of sensors, which are not always available in real-world applications, an alternative configuration based on a multi-setup approach was also considered and tested [33]. In this configuration, six different setups were used: two sensors were kept fixed as reference points, while the remaining five sensors were sequentially repositioned along the structure to acquire data over its entire length. This approach allowed the acquisition of equivalent information corresponding to 32 measurement points by using only seven accelerometers in total. The results of the MAC-based comparison between the experimental data for the D3 damage case, obtained using the single-setup configuration and the multi-setup configuration, are presented in Fig. 6.

The mode shapes obtained from the two configurations are almost identical, and consequently, the results of the damage detection analysis are expected to be very similar. However, the results presented in this work, in Section 4, refer to the mode shapes derived from the single-setup configuration.

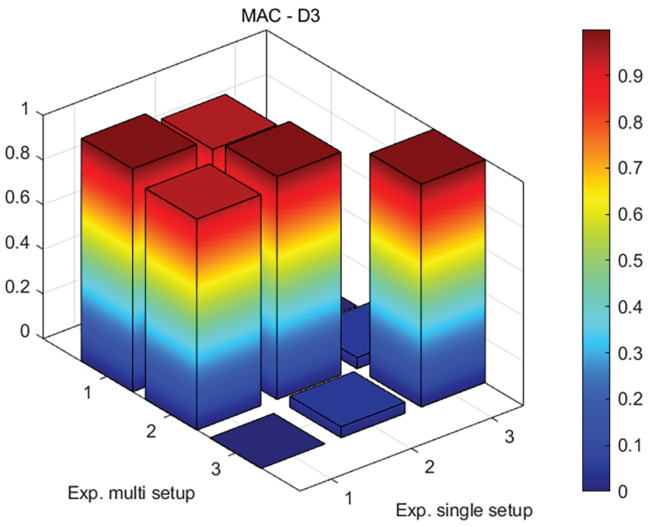

Figure 6: MAC comparison between single setup and multi setup configuration for D3 damage case

Table 5 shows the quantitative results of the MAC value.

Table 5: MAC values between the experimental mode shapes obtained with a single setup and a multi-setup configuration for the D3 damage case

D3 Case		Single setup		
		1st Mode (bending)	2nd Mode (torsional)	3rd Mode (bending)
Multi-setup	1st Mode (bending)	1.0000	0.9498	0.0000
	2nd Mode (torsional)	0.9467	0.9999	0.0499
	3rd Mode (bending)	0.0000	0.0492	0.9996

4 Damage Localization Results

The method outlined in Section 2 was applied to the identified mode shapes. Specifically, the proposed concept of using the first derivative of the first torsional mode shape, supported by the application of the Continuous Wavelet Transform (CWT), to localize the damage, was implemented and compared with the traditional curvature-based method, which applies the second derivative to the second bending mode shape.

Due to its geometry, the LUMO structure exhibited mode shapes that were almost completely decoupled. Fig. 7a,b, respectively, show the damage localization results obtained from the torsional and bending mode shapes for the D1 damage case. Similarly, the results for the D2 and D3 cases are presented in Figs. 8 and 9, respectively. In all graphs, the regions affected by damage are highlighted.

As shown in Figs. 7–9, the method based on the use of the first derivative successfully and clearly localized the damage in at least two of the three analyzed cases, D1 and D2. For the third case, D3, a pronounced peak, even if not so much higher than the others, is observed near the damaged region; however, it is not perfectly contained within it. In contrast, when applying the curvature-based method, a peak is visible only for the D1 case.

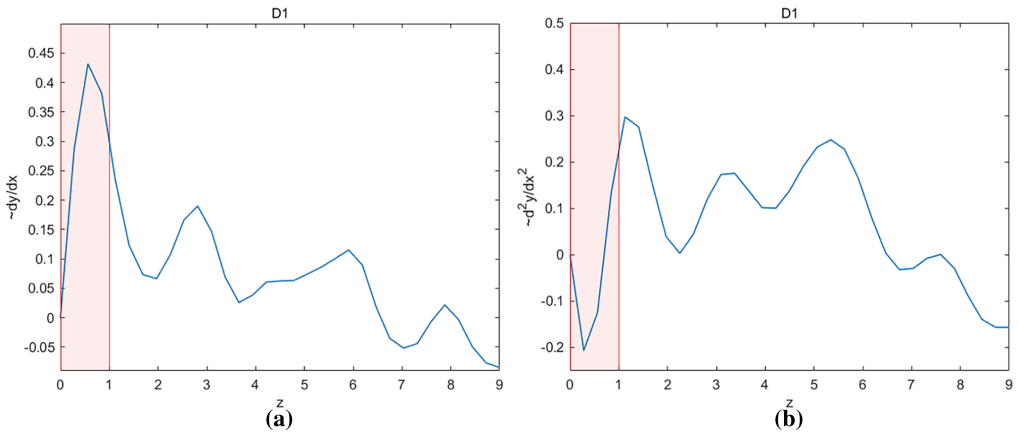

Figure 7: Damage localization results for D1 case with the first derivative method (**a**) and the curvature method (**b**)

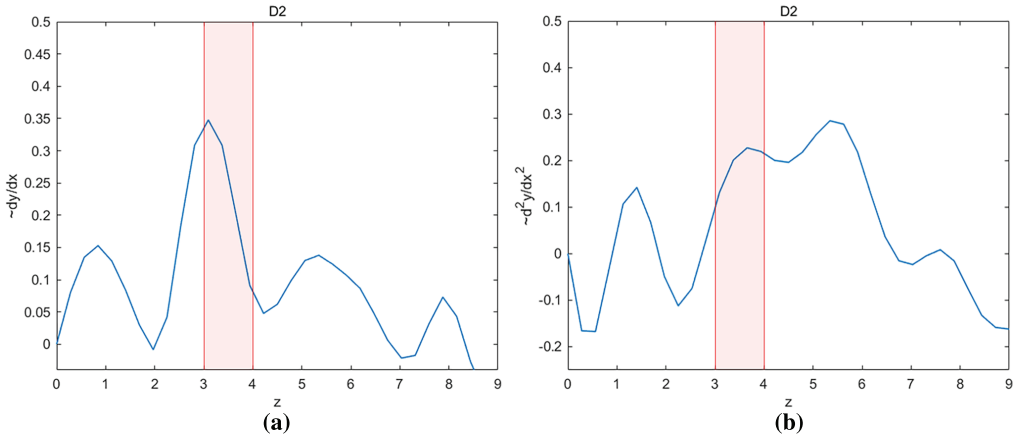

Figure 8: Damage localization results for D2 case with the first derivative method (**a**) and the curvature method (**b**)

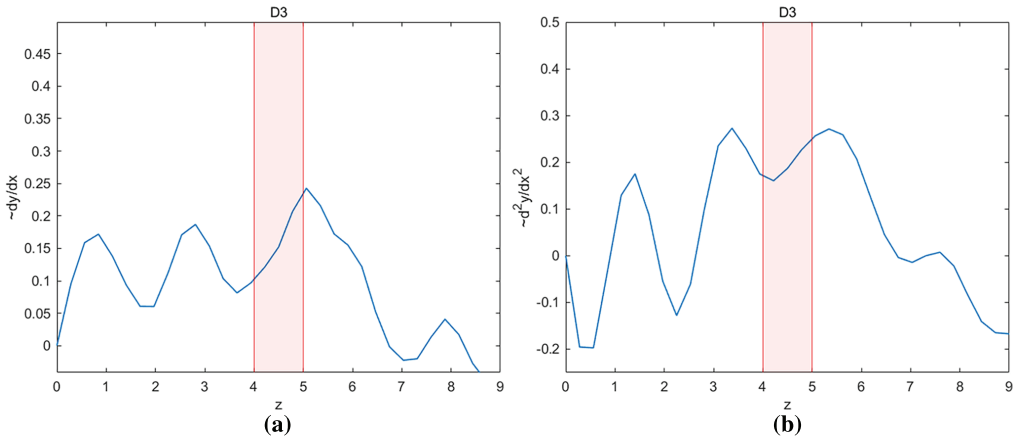

Figure 9: Damage localization results for D3 case with the first derivative method (**a**) and the curvature method (**b**)

To better understand the superior performance of the first derivative for the analyzed truss structure, an index was introduced to quantify the accuracy of the two damage-localization methods. Specifically, the accuracy was evaluated by measuring the deviation between the peak in the derivative and the actual damaged area. This deviation, expressed in meters, is reported as the index δ in Table 6.

Table 6: Accuracy indexes of damage localization obtained with 1st and 2nd derivatives for all the damaged cases

	δ [m]-D1	δ [m]-D2	δ [m]-D3
1st Derivative	0	0	0.04
2nd Derivative	0	1.34	0.34

As can be seen from Table 6, with the use of the 1st derivative method, the peak related to the localization of damage is almost always contained in the highlighted damaged area, while the use of the 2nd derivative leads to a huge error, especially considering that for D2 and D3 cases there is not a clear peak that was more visible than the others.

5 Conclusions

Building on the well-known curvature method used for damage detection and localization, typically applied to bending mode shapes, the goal of this study was to extend this approach by demonstrating not only how torsional mode shapes and their first derivatives can be used to detect and locate damage, but also that, in some cases, this extended method provides better results than the classical curvature technique. Consequently, it becomes important to incorporate this approach into damage detection analyses based on mode-shape derivatives, and in particular to employ both methods when dealing with real-world structures. This is because, in practical applications, pure bending modes are not always guaranteed; geometric and material characteristics may lead to mode shapes that are predominantly bending or predominantly torsional. In such cases, considering the first derivative (slope) of the torsional mode shape becomes essential. Moreover, the lower sensitivity of the first derivative, compared to the second derivative, to spurious peaks induced by noise in experimental data must also be considered as another advantage.

To achieve this goal, an appropriate experimental campaign was designed and conducted on a real-world truss structure. The collected data allowed for the identification of the first and second bending modes and the first torsional mode shape of the structure. Visual results of the obtained derivatives, as well as an introduced accuracy index, demonstrate how applying the first- and second-derivative methods revealed that using the first derivative on the torsional mode shape produced better results, enabling damage detection and clear damage localization in at least two of the three cases analyzed.

Moreover, a clear advantage of the introduced method was that the described results were obtained using ambient vibration data acquired over a duration of only 10 min per test, with 32 non-equidistant measurement points.

Finally, a multi-setup approach was tested and compared with the single-setup configuration, providing an alternative strategy for conducting measurements when a large number of sensors is not available.

The method was tested on a truss structure in operating conditions, so subjected to environmental conditions, showing the robustness of the method against ambient and measurement noise. Future research could extend its applicability to different types of structures.

Acknowledgement: Many thanks to the Statik und Dynamik research group of the Leibniz University of Hannover for the availability and support in conducting the new measurements on the LUMO structure.

Funding Statement: The authors received no specific funding for this study.

Author Contributions: The authors confirm contribution to the paper as follows: Conceptualization, Giada Faraco and Arcangelo Messina; methodology, Giada Faraco; software, Giada Faraco; validation, Giada Faraco; formal analysis, Giada Faraco; investigation, Giada Faraco; data curation, Giada Faraco; writing—original draft preparation, Giada Faraco; writing—review and editing, Giada Faraco and Nicola Ivan Giannoccaro; visualization, Giada Faraco and Andrea Vincenzo De Nunzio; supervision, Nicola Ivan Giannoccaro; project administration, Andrea Vincenzo De Nunzio and Arcangelo Messina. All authors reviewed the results and approved the final version of the manuscript.

Availability of Data and Materials: Data available on request from the authors. The data that support the findings of this study are available from the Corresponding Author, [Giada Faraco], upon reasonable request.

Ethics Approval: Not applicable.

Conflicts of Interest: The authors declare no conflicts of interest to report regarding the present study.

References

1. Government of India C Electricity Authority. Report of the standing commitee of experts on failure of EHV transmission line towers. New Delhi, India: Central Electricity Authority (Government of India); 2018.
2. Sun X, Ilanko S, Mochida Y, Tighe RC. A review on vibration-based damage detection methods for civil structures. Vibration. 2023;6(4):843–75. doi:10.3390/vibration6040051.
3. Dessi D, Camerlengo G. Damage identification techniques via modal curvature analysis: overview and comparison. Mech Syst Signal Process. 2015;52–53(2):181–205. doi:10.1016/j.ymssp.2014.05.031.
4. Mengesha G. Integrating AI in structural health monitoring (SHM): a systematic review on advances, challenges, and future directions [Internet]. SSRN; 2025 [cited 2025 Oct 24]. Available from: https://www.ssrn.com/abstract=5004977.
5. Nguyen DH, Nguyen QB, Bui-Tien T, De Roeck G, Abdel Wahab M. Damage detection in girder bridges using modal curvatures gapped smoothing method and convolutional neural network: application to Bo Nghi bridge. Theor Appl Fract Mech. 2020;109(3–4):102728. doi:10.1016/j.tafmec.2020.102728.
6. Nguyen DH, Abdel Wahab M. Damage detection in slab structures based on two-dimensional curvature mode shape method and Faster R-CNN. Adv Eng Softw. 2023;176(5):103371. doi:10.1016/j.advengsoft.2022.103371.
7. Römgens N, Abbassi A, Jonscher C, Grießmann T, Rolfes R. On using autoencoders with non-standardized time series data for damage localization. Eng Struct. 2024;303(4):117570. doi:10.1016/j.engstruct.2024.117570.
8. Wickramarachchi CT, Gardner P, Poole J, Hübler C, Jonscher C, Rolfes R. Damage localisation using disparate damage states via domain adaptation. Data-Centric Eng. 2024;5:e3. doi:10.1017/dce.2023.29.
9. Ragnitz J, Hofmeister B, Jonscher C, Hübler C, Rolfes R. A stochastic multi-objective optimisation approach for damage localisation via model updating with uncertain input parameters. Eng Struct. 2025;330(2):119860. doi:10.1016/j.engstruct.2025.119860.
10. Thurn J, Kullaa J, Jonscher C, Rolfes R. Autocovariance functions as damage sensitive features: case study of a lattice tower. Cham, Switzerland: Springer; 2025.
11. Pandey AK, Biswas M, Samman MM. Damage detection from changes in curvature mode shapes. J Sound Vib. 1991;145(2):321–32. doi:10.1016/0022-460x(91)90595-b.
12. Ratcliffe CP. Damage detection using a modified laplacian operator on mode shape data. J Sound Vib. 1997;204(3):505–17. doi:10.1006/jsvi.1997.0961.
13. Gentile A, Messina A. On the continuous wavelet transforms applied to discrete vibrational data for detecting open cracks in damaged beams. Int J Solids Struct. 2003;40(2):295–315. doi:10.1016/s0020-7683(02)00548-6.
14. Messina A. Detecting damage in beams through digital differentiator filters and continuous wavelet transforms. J Sound Vib. 2004;272(1–2):385–412. doi:10.1016/j.jsv.2003.03.009.
15. Yazdanpanah O, Seyedpoor SM, Bengar HA. A new damage detection indicator for beams based on mode shape data. Struct Eng Mech. 2015;53(4):725–44.

16. Lima Júnior WJD, Assis WSD. A modified mode shape data-based method for beams structural damage detection. Acta Sci Technol. 2023;45:e63847. doi:10.4025/actascitechnol.v45i1.63847.
17. Roy K, Ray-Chaudhuri S. Fundamental mode shape and its derivatives in structural damage localization. J Sound Vib. 2013;332(21):5584–93. doi:10.1016/j.jsv.2013.05.003.
18. Ren X, Meng Z. Damage identification for timber structure using curvature mode and wavelet transform. Structures. 2024;60(1):105798. doi:10.1016/j.istruc.2023.105798.
19. Porcu MC, Patteri DM, Melis S, Aymerich F. Effectiveness of the FRF curvature technique for structural health monitoring. Constr Build Mater. 2019;226(4):173–87. doi:10.1016/j.conbuildmat.2019.07.123.
20. Sokhangou F, Sorelli L, Chouinard L, Dey P, Conciatori D. Detecting multiple damages in UHPFRC beams through modal curvature analysis. Sensors. 2024;24(3):971. doi:10.3390/s24030971.
21. Rucevskis S, Wesolowski M. Identification of damage in a beam structure by using mode shape curvature squares. Shock Vib. 2010;17(4–5):601–10. doi:10.1155/2010/729627.
22. He M, Yang T, Du Y. Nondestructive identification of composite beams damage based on the curvature mode difference. Compos Struct. 2017;176(1):178–86. doi:10.1016/j.compstruct.2017.05.040.
23. Cao MS, Xu W, Ren WX, Ostachowicz W, Sha GG, Pan LX. A concept of complex-wavelet modal curvature for detecting multiple cracks in beams under noisy conditions. Mech Syst Signal Process. 2016;76–77:555–75. doi:10.1016/j.ymssp.2016.01.012.
24. Pooya SMH, Massumi A. A novel and efficient method for damage detection in beam-like structures solely based on damaged structure data and using mode shape curvature estimation. Appl Math Model. 2021;91(4):670–94. doi:10.1016/j.apm.2020.09.012.
25. Sung SH, Jung HJ, Jung HY. Damage detection for beam-like structures using the normalized curvature of a uniform load surface. J Sound Vib. 2013;332(6):1501–19. doi:10.1016/j.jsv.2012.11.016.
26. Whalen TM. The behavior of higher order mode shape derivatives in damaged, beam-like structures. J Sound Vib. 2008;309(3–5):426–64. doi:10.1016/j.jsv.2007.07.054.
27. Garrido H, Domizio M, Curadelli O, Ambrosini D. Numerical, statistical and experimental investigation on damage quantification in beams from modal curvature. J Sound Vib. 2020;485(3):115591. doi:10.1016/j.jsv.2020.115591.
28. Roy K. Structural damage identification using mode shape slope and curvature. J Eng Mech. 2017;143(9):04017110. doi:10.1061/(asce)em.1943-7889.0001305.
29. Huang Z, Zang C. Damage detection using modal rotational mode shapes obtained with a uniform rate CSLDV measurement. Appl Sci. 2019;9(23):4982. doi:10.3390/app9234982.
30. Xu W, Zhu WD, Smith SA, Cao MS. Structural damage detection using slopes of longitudinal vibration shapes. J Vib Acoust. 2016;138(3):034501. doi:10.1115/1.4031996.
31. Araújo Dos Santos JV, Lopes HMR, Ribeiro J, Maia NMM, Pires Vaz MA. Damage localisation in beams using the ritz method and speckle shear interferometry. In Valencia, Spain; [cited 2025 Oct 28]. p. 54. Available from: http://www.ctresources.info/ccp/paper.html?id=5761.
32. Hearn EJ. Mechanics of materials: an introduction to the mechanics of elastic and plastic deformation of solids and structural materials. 3rd ed. Vol. 1. Oxford, UK: Butterworth-Heinemann; 1997.
33. Faraco G, De Nunzio AV, Giannoccaro NI, Messina A. A non-destructive approach for damage localization in civil or mechanical structures without reference model. In: Caetano E, Cunha Á, editors. Experimental vibration analysis for civil engineering structures. Cham, Switzerland: Springer Nature; 2025 [cited 2025 Oct 28]. p. 671–80. (Lecture Notes in Civil Engineering; Vol. 674). Available from: https://link.springer.com/10.1007/978-3-031-96110-6_65.
34. Institut für Statik und Dynamik. Leibniz universitat hannover [Internet]. [cited 2025 Jan 1]. Available from: https://www.isd.uni-hannover.de/de/.
35. Wernitz S, Hofmeister B, Jonscher C, Grießmann T, Raimund R. A new open-database benchmark structure for vibration-based Structural Health. Struct Control Health Monit. 2022;29(11):e3077. doi:10.1002/stc.3077.
36. ARTeMIS Modal [Internet]. Structural Vibration Solutions. [cited 2025 Jan 1]. Available from: https://www.svibs.com/artemis-modal/.

37. Khanahmadi M, Gholhaki M, Rezaifar O, Dezhkam B. Signal processing methodology for detection and localization of damages in columns under the effect of axial load. Measurement. 2023;211(23):112595. doi:10.1016/j.measurement.2023.112595.
38. Khanahmadi M, Mirzaei B, Ghodrati Amiri G, Gholhaki M, Rezaifar O. A numerical study on vibration-based interface debonding detection of CFST columns using an effective wavelet-based feature extraction technique. Steel Compos Struct. 2024;53(1):45–59.